Tehran University of Medical Sciences Publication
http://tums.ac.ir

Iran J Parasitol

Open access Journal at
http://ijpa.tums.ac.ir

Iranian Society of Parasitology
http://isp.tums.ac.ir

Original Article

Microfluidic-Synthesized Chitosan Nanoparticles Loaded with Azithromycin: Impact on *Toxoplasma gondii* Tissue Cysts in Mouse Model

Mohammad Mahdi Heidari [1], *Asghar Fazaeli [1], Samad Nadri [2], Negin Torabi [1], Mehrzad Saraei [3]

1. *Department of Parasitology and Mycology, School of Medicine, Zanjan University of Medical Sciences, Zanjan, Iran*
2. *Department of Medical Nanotechnology, School of Medicine, Zanjan University of Medical Sciences, Zanjan, Iran*
3. *Department of Parasitology and Mycology, School of Medicine, Qazvin University of Medical Sciences, Qazvin, Iran*

Received 12 Jun 2024
Accepted 19 Oct 2024

Keywords:
Toxoplasma gondii;
Tissue cyst;
Azithromycin;
Chitosan;
Nanoparticles

***Correspondence**
Email:
fazaeli@zums.ac.ir

Abstract

Background: We aimed to investigate the effect of chitosan nanoparticles loaded azithromycin on reducing the number of *Toxoplasma gondii* tissue cysts in the brain of a mouse model.

Methods: Chitosan nanoparticles and azithromycin loaded nanoparticles were synthesized using microfluidic system and characterized using dynamic light scattering (DLS) and TEM images. Forty BALB/c mice after infection with a cyst forming *T. gondii* strain, were divided into four groups daily receiving PBS, 10 mg/kg azithromycin, 10 mg/kg chitosan nanoparticles, and 10 mg/kg chitosan nanoparticles loaded azithromycin, respectively, for 10 days. Immediately after end of the treatment, the mice were sacrificed and the tissue cyst burden in their brain was investigated using an optical microscope and compared by ANOVA statistical test.

Results: The average particle size and dispersion index for chitosan nanoparticles were 193.66 nm and 0.43, and for nanoparticles containing azithromycin drug, they were 233.66 nm and 0.21, respectively. The amount of drug loading was 1.8% and the drug release was more than 90% after less than 48 hours. The stability of nanoparticles did not change significantly after 28 days of observation. *Toxoplasma* tissue cyst numbers obtained in a range of 1.48 to 1.95 in 10 ul brain suspension with no significant differences among the groups of treated mice.

Conclusion: The synthesis of chitosan nanoparticles loaded with azithromycin by microfluidic system could make the particles with more uniformity and stability and high loading of the drug with low cost and more convenient conditions.

Introduction

Toxoplasmosis, caused by the intracellular parasitic protozoan *Toxoplasma gondii*, is a significant infection transmitted through various routes, particularly by consuming undercooked meats and meat products (1,2). In chronic form, the parasites exist as tissue cysts containing numerous bradyzoites, primarily forming in the brain, central nervous system (CNS), eyes, smooth and skeletal muscles, and occasionally in other organs like the kidneys and liver. When the immune system is compromised, bradyzoites can transform into tachyzoites, reactivating into an acute infection (3). Chronic toxoplasmosis, associated with tissue cysts, has been linked to neurological disorders such as schizophrenia and behavioral issues (4-7).

Tissue cysts are resistant to immune responses, and no approved treatment can completely eliminate them from the body (8, 9). Azithromycin, a macrolide antibiotic, can affect both acute and chronic forms of toxoplasmosis (10-14). Nanotechnology in drug delivery involves designing nanoparticles (NPs) and nanosystems to efficiently deliver drugs to specific body sites (15, 16). These NPs, ranging from 10-1000 nanometers, can be made from various materials and offer advantages like drug encapsulation, protection from degradation, enhanced solubility, and controlled release. Functionalized NPs can target specific cells or tissues, improving drug concentration at the desired site while minimizing side effects on healthy cells (17, 18).

Microfluidics, a method involving small channels to handle and manipulate fluids, offers advantages over traditional bulk synthesis methods for creating NPs. This technique provides precise control, rapid mixing, scalability, continuous production, and integration with other processes (19). Chitosan, a natural polymer derived from chitin found in crustacean exoskeletons, is biocompatible, biodegradable, and suitable for producing nanoparticles with specific drug release profiles (20-24). Its antimicrobial effect was investigated in several infectious organisms including protozoan parasites.

Metronidazole-loaded chitosan NPs were evaluated against *Giardia lamblia* infection in Syrian hamsters and enhanced the therapeutic effect compared to metronidazole alone (23). Studies on the anti-*Toxoplasm* effect of chitosan NPs have mostly been conducted on the RH strain or on the tachyzoite stage of the parasite. For example, Teimouri et al., (25) evaluated different concentrations of chitosan against tachyzoites of *Toxoplasma* RH strain *in vitro* and *in vivo* with satisfactory efficacy.

Few studies have been done on anti-toxoplasma compounds in the cyst stage of the parasite. Saraei et al investigated the effect of aripiprazole on tissue cysts in the mouse brain and did not observe any reduction in parasite cysts (26). In another study using fluphenazine and thioridazine against tissue cysts of *Toxoplasma* Tehran strain in mice, cytogenesis in the brain of infected animals was not inhibited (27).

The present study was designed to investigate the effect of chitosan nanoparticles loaded azithromycin on reducing the number of *T. gondii* tissue cysts in the brain of a mouse model.

Materials and Methods

Making microfluidic system to prepare nanoparticles

A microfluidic system was created using a polydimethylsiloxane (PDMS) chip (obtained from Riz Tarashe Mizan Company, Karaj, Iran). The chip design included input, passage, and output channels for nanoparticles. It was designed with Solidworks software and printed onto a mask. A silica wafer (Riz Tarashe Mizan Co.) was prepared as the stationary phase. Su-8 (Riz tarashe Mizan Co.), a light-

sensitive polymer, was applied to the wafer and cured using UV irradiation through the mask. The uncured parts were dissolved, leaving the original design. PDMS and its cross-linker were applied to the slide and heated to form the structure. Input and output channels were then punched into the mold (23, 28).

Preparation of chitosan polymer and chitosan-azithromycin solution

A chitosan polymer solution (high molecular weight, 75% deacetylation, Sigma-Aldrich) was prepared by dissolving 20 mg of chitosan powder in 1% acetic acid and stirring overnight. Azithromycin powder (Daroupakhsh Shimi, Tehran, Iran) was added to this solution to create the drug solution. A stock solution of tripolyphosphate (TPP) was prepared with various dilutions. Tween 80 was dissolved in deionized water and, if necessary, sodium hydroxide (NaOH) was used to adjust the pH (23).

Synthesis of chitosan nanoparticles and drug loaded nanoparticles

To synthesize NPs, the microfluidic system was connected to two syringe pumps. The polymer and azithromycin solution was pumped at a flow rate of 5 mm/hr, while the Tween 80 and tripolyphosphate solution was pumped at flow rates of 5 and 2.5 mm/hr. The solution containing NPs and drug was then subjected to sonication for 30 minutes (19, 20, 23).

Physicochemical characterization of the prepared nanoparticles

The size and polydispersity index (PDI) of the nanoparticles were measured using dynamic light scattering (DLS) with a Nano Zeta sizer. The process was repeated three times, and the results were reported as mean values ± standard deviations. To examine the shape of NPs, TEM image of synthesized NPs was obtained at the Central Materials Engineering Laboratory of Khajeh Nasiruddin Tusi University (Tehran, Iran).

Determination of drug loading and stability test

The drug loading efficiency refers to the ratio of the drug content incorporated within the nanoparticle structure to the total weight of the nanoparticle. To determine the drug loading efficiency, the following steps were performed after synthesizing the drug nanoparticles. The resulting solution was subjected to centrifugation. The supernatant was then discarded, and the tube containing the nanoparticle sediment was incubated at 37 °C for 24 hours. The weight of the sediment was measured using a precise scale. To break down the NPs, the sediment was sonicated at high speed for one hour. A portion of the supernatant solution was used for the measurement of its absorption value using a spectrophotometer. The amount of drug loading was then calculated using the calibration curve (19). In order to assess the stability of the nanoparticle size, the size of the synthesized NPs was measured at specific time intervals including 1, 7, 14, 21 and 28 days with 3 repetitions.

Measurement of drug release rate in vitro

Drug-loaded NPs were sealed in a dialysis bag and immersed in a Falcon tube with 10 ml of PBS solution and 2% Tween 80. The tube was placed in a shaker incubator at 37 °C with a rotation speed of 100 rpm for a week. At specific intervals, 500 µl of the solution was replaced with fresh PBS to measure drug release using a spectrophotometer at a wavelength of 226 nm.

Animals

Forty-five female BALB/c mice, aged 7-8 weeks and weighing 20-25 grams, were purchased from Karamad Zist Exir Company, Teharn, Iran. They were kept at Zanjan University's lab animal care center under standard conditions, following the guidelines provided by the National Ethics Committee for Working with Laboratory Animals. This research was approved by the Ethics Committee of

Zanjan University of Medical Sciences (code: IR.ZUMS.REC.1400.327). The conditions included a temperature of 25 °C, a 12-hour light-dark cycle, and free access to food and water.

Parasite strain and tissue cyst inoculation in mice

Two mice infected with tissue cysts of the *T. gondii* Tehran strain, which is a tissue cyst forming type II strain, were gifted from the Department of Parasitology at Tehran University of Medical Sciences, Tehran, Iran. For the primary passage to produce sufficient parasite stock, a suspension containing tissue cysts was intraperitoneally inoculated into 5 mice using 0.5 ml per mouse containing approximately 20 cysts. Following a 3-month period in the subsequent passage, during which a satisfactory number of cysts formed in the mice brains, an adequate suspension amount was prepared for inoculating the various test groups. Each mouse of the treatment and control groups was intraperitoneally inoculated with 0.5 ml (~ 20 tissue cysts) (27).

After confirming the formation of tissue cysts in the brains of mice by randomly examining the brains of a number of mice, 120 days post-infection, the mice were randomly assigned to four groups of 10 each, and subsequently received daily intraperitoneal injection as follows: control Group received 0.5 ml PBS only. Azithromycin Group received 0.5 ml PBS containing 10 mg/kg of azithromycin, Chitosan NPs (Ch) Group received 0.5 ml PBS containing 10 mg/kg of chitosan. Azithromycin loaded chitosan NPs (AZM-Ch) Group received 0.5 ml PBS containing 10 mg/kg of azithromycin loaded chitosan NPs. Based on previous studies, the treatment duration for all groups was set at 10 days (26, 27).

Evaluation of treatment effect and data analysis

Post-treatment, mice were anesthetized and their brains were isolated and homogenized and tissue cysts were counted (29). Cyst counts from different groups were compared using a one-way ANOVA test.

Results

The microfluidic system, created using soft lithography, optimally uses a 1 mg/ml polymer solution and a 4 mg/ml drug-infused polymer solution. The ideal concentration for the tripolyphosphate (TPP) solution, which affects nanoparticle size, is also 1 mg/ml at a flow rate of 5 ml/h.

Table 1 presents the size of nanoparticles and their dispersion index. Additionally, we calculated the drug loading in the NPs, and it was 1.8% based on drug calibration curve (Fig. 1). The formation of NPs was further confirmed through electron microscopic images (Fig. 2), which showed that the size and morphology of the nanoparticles were consistent with the results obtained from DLS measurements (Fig. 3).

Nanoparticle stability, assessed over 28 days, showed no significant changes in size or PDI (Table 2).

Table 1: Size and poly dispersion index of chitosan nanoparticles and azithromycin loaded nanoparticles

Nanoparticles	Mean Size (nm)	PDI*
Chitosan NPs	193.66	**0.4**
Azithromycin loaded NPs	**233.66**	**0.2**

*PDI (poly dispersion index) less than 0.5 indicates homogenous nature of formulation

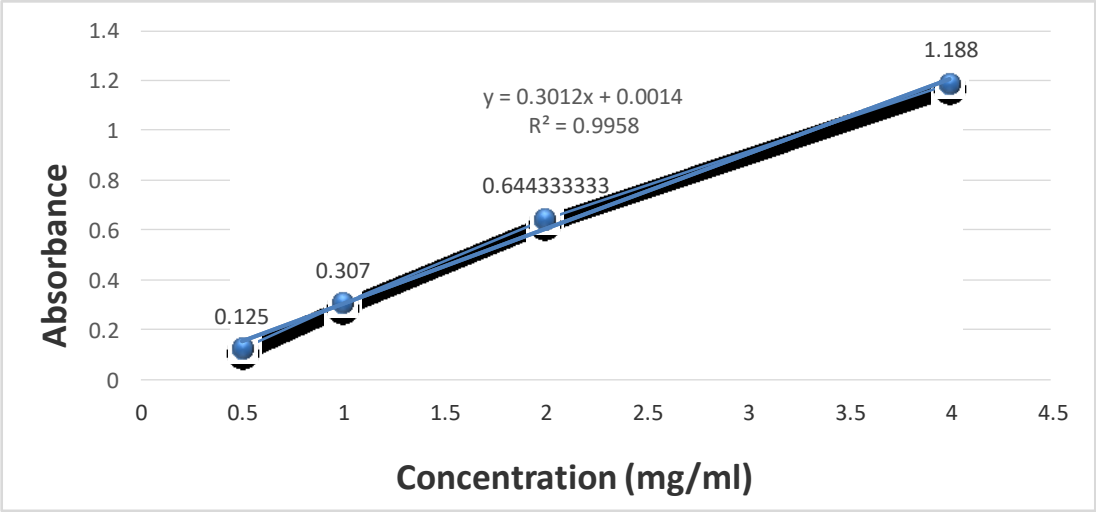

Fig. 1: Azithromycin drug calibration curve at the maximum wavelength of 226 nm (98% ethanol solvent)

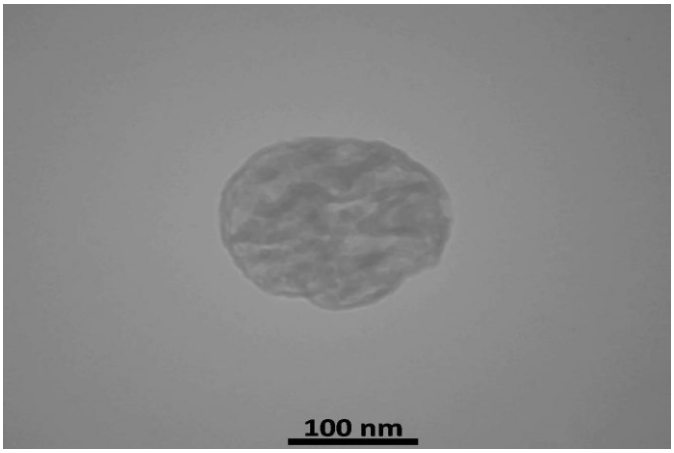

Fig. 2: Electron microscope image of nanoparticles synthesized by the microfluidic system

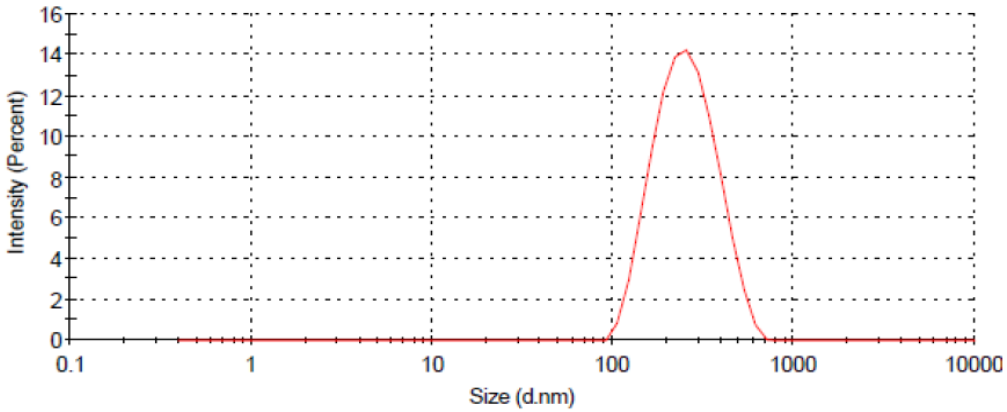

Fig. 3: Particle size distribution diagram of chitosan nanoparticles loaded with azithromycin

Table 2: Average size of chitosan nanoparticles and poly dispersion index during 28 days

Time (day)	Size (nm) ± SD	PDI
1	230.9 ± 10.51	0.2
7	258 ± 6.02	0.2
14	237.76 ± 8.55	0.19
21	248.6 ± 12.2	0.2
28	**258 ± 9**	**0.4**

In vitro release test

The drug release data indicated a rapid release pattern of azithromycin, with over 80% release within the first 24 h. Subsequently, it reached its maximum release rate of 100% by 72 h, and the graph showed a plateau until the end of the 7th day (Fig. 4).

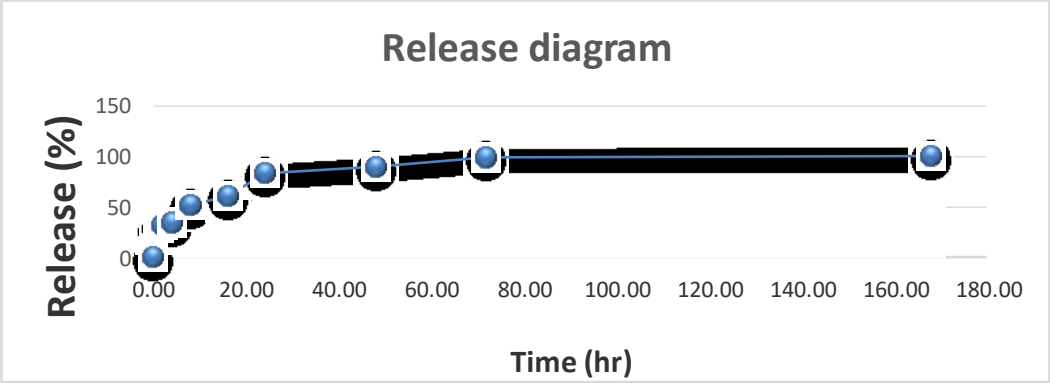

Fig. 4: Drug release from chitosan nanoparticles loaded with azithromycin

Effect of chitosan nanoparticles containing azithromycin on the number of brain cysts

The average number of *T. gondii* tissue cysts in different study groups of mice are shown in Table 3. A sample of tissue cysts in brain is shown in Fig. 5.

Table 3: The average number of *Toxoplasma gondii* tissue cysts in different groups of mice

Experimental groups (n=10/group)	Cyst number/10 µl * (mean)	SD
PBS (untreated control)	1.86	1.42
Ch nanoparticles	1.48	0.53
AZM	1.90	0.86
AZM-Ch nanoparticles	**1.95**	**1.83**

*In the volume of 10 microliters of the brain suspension. Ch, chitosan; AZM, azithromycin; AZM-Ch, azithromycin-loaded chitosan

Through statistical comparison, it was determined that the number of cysts in the four studied groups did not exhibit significant difference.

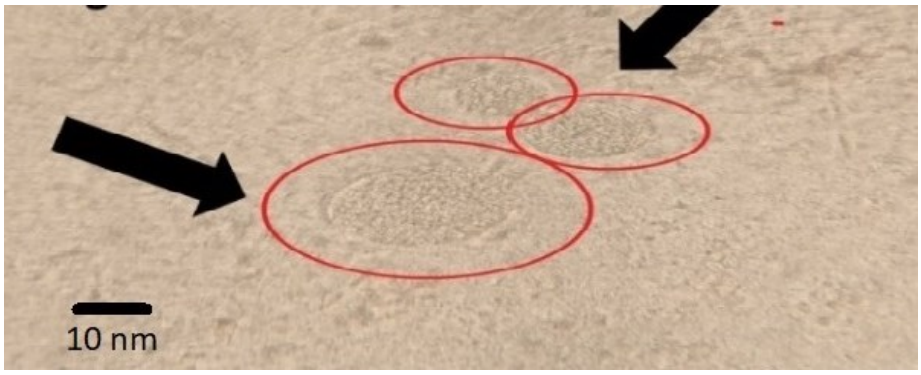

Fig. 5: Image of tissue cysts of *Toxoplasma gondii* under a light microscope magnification with 40x lens

Discussion

This study showed that synthesizing chitosan NPS loaded with azithromycin using a microfluidic system produced uniform, suitable particles with high drug loading at low cost. However, a 10 mg/kg dose did not significantly reduce tissue cysts in infected mice. Nanoparticle size was influenced by flow rate and solution concentration, with an optimal flow rate of 5 ml/h producing smaller, uniform NPS. Excessive flow rates and higher tripolyphosphate concentrations resulted in larger nanoparticles. The average size of the nanoparticles was 193.66 nm, increasing to 233.66 nm after drug loading, aligning with previous research. Electron microscopy confirmed the expected morphology and traits. The mean cyst count in the nanoparticle-treated group was 1.95, compared to 1.86 in the control group, with no significant difference.

Some researchers conducted similar studies, but they mainly targeted the tachyzoite stage, which represents the acute form of *Toxoplasma* infection. Teimouri and colleagues evaluated different concentrations of Cs against *Toxoplasma* RH strain *in vitro* and *in vivo* and reported satisfactory efficacy. However, they treated the tachyzoite stage of the parasite, which is not comparable to the chronic tissue cyst form (25). In another study, low molecular weight Cs against *Plasmodium braghei* was used in a mouse model, which resulted in longer survival of treated mice. It goes without saying that this active parasite in the blood can easily be exposed to the inoculated therapeutic compounds. Meanwhile, the *Toxoplasma* cyst, which is a latent stage in tissue, is not readily available for compounds (30). Gaffar et al., showed that chitosan and silver NPS were effective against experimental toxoplasmosis in mice. Again, this experiment was performed on the tachyzoite stage, which is an active proliferative form and completely different from the tissue cyst stage (31). The effectiveness of different concentrations of chitosan with low molecular weight against *Toxoplasma* tachyzoites has been reported with good results (32). *In vitro* exposure of tachyzoites to chitosan cannot be a suitable model to evaluate drugs against this parasite, especially its chronic form.

A study by Soheili et al. which employed soft lithography technology for a microfluidic system, emphasized the significant role of incorporation speed in chitosan nanoparticle synthesis as drug carriers (19). This speed critically influences both drug loading extent and subsequent release rate. Consequently, meticulous attention to the system's initial configuration, encompassing factors such as channel diameter and length, emerges as imperative within this realm.

Within the current microfluidic setup, adopting a Y-shaped design has yielded smaller nanoparticles while preserving effective

drug loading. Based on the diagram derived from the data, the drug release profile illustrates that over 90% of the drug was discharged within 48 hours. This pattern aligns with the findings of Raouf et al., where nearly the entire drug load was released within the same 48-hour timeframe (33).

Exploration of nanoparticle stability has revealed periods of stability up to 28 days. This corresponds with the findings of a study by Jonassen et al., which explored the stability of chitosan nanoparticles under varied conditions and identified their stability over a month (34). Similarly, in a research by Habibzadeh et al., focusing on nanoparticles synthesized through a microfluidic system, demonstrated consistent size and zeta potential over a span of 30 days, devoid of significant variations (35).

For quantification of tissue cysts we followed the protocol outlined by Abd Elgaward et al (29). This process involved homogenizing mouse brains with PBS, generating a suspension subsequently used to prepare at least 3 slides per sample, each containing 10 microliters. These slides were subjected to examination under a 40× objective lens of an optical microscope. Diverse methods have been employed for tissue cyst enumeration across various studies. For instance, Dumas et al employed a technique where the prepared suspension was subjected to centrifugation, enhancing the likelihood of detecting all tissue cysts within a smaller sample volume under a light microscope (36).

Within the context of nanoparticle synthesis using microfluidics, notable achievements were realized, particularly in achieving a substantial drug loading of 1.8%. The Polydispersity Index that quantifies particle size dispersion generally tended to be higher in this method. Studies by Hagras et al. and Etewa et al. (22, 24) diverged from this approach, adopting conventional bulk methods for solution merging

The high molecular weight chitosan was used in our study. Teimouri et al. suggest lower molecular weights are more effective, potentially impacting our carrier's efficacy (25).

In the present study, Tehran strain of *T. gondii* was used, which is different from the strains employed in most comparable investigations (11, 12, 22, 37, 38). These studies commonly utilized the Me49 strain (32). Hence, discrepancies in results could potentially stem from variations in the strains studied. In a couple of studies, focusing on the Tehran strain, the authors similarly did not yield the expected effects on tissue cysts decrease in mouse models (26, 27).

The treatment period in our current study spans 10 days, a duration comparable to several influential prior investigations. For instance, Djurković et al. applied clindamycin over a 3-month course (39). Ferreira et al. evaluated sulfadiazine and combination therapies over 4 weeks (40). Shu and Jiang et al. investigated minocycline for 3 weeks (41), while Ferguson et al. studied atovaquone for a month in 1994 (42). Notably, certain studies, adopted shorter durations, achieving effective outcomes over 8 days (43, 44). Chew et al. also demonstrated effectiveness with a 7-day regimen involving spiramycin (45).

Given the challenges linked with macrolide antibiotics like azithromycin crossing the blood-brain barrier, the utilization of suitable carriers such as chitosan has been proposed to mitigate required dosages (40). However, a precise dose for loading azithromycin onto a chitosan carrier to impact brain tissue in mice remains undetermined. Raouf et al. reported the effectiveness of a 10 mg/kg/day dose against *Pseudomonas* bacteria biofilm in mice model (33).

In the existing studies, as previously mentioned, dosages of 100, 200, 250, and 300 mg/kg/day have been explored. Most of these investigations focused on the RH strain during its acute phase and did not involve drug carriers (46). In contrast, our current study employed a dosage lower than the LD50 value

(lethal dose for 50% of subjects) of azithromycin (10 mg/kg/day) in mice.

In this investigation, the drug was administered via the intraperitoneal route. Similarly, Raouf et al. introduced azithromycin nanoparticles through intraperitoneal injections in Syrian mice (33). Whereas, Dumas et al. employed an oral administration of the drug in their study focused on tissue cysts (36). Degerli's study, which focused on the acute phase of the disease, also administered the drug orally (13).

Several factors might contribute to these results, including the limitations for production nanoparticles with high loading drug in this system, which may hinder the administration of higher doses. The duration of the treatment (10 days), the injection dose of azithromycin, the intraperitoneal administration of drug, and the possibility of drug resistance could have further impacted the results obtained.

Conclusion

The synthesis of chitosan nanoparticles loaded with azithromycin by microfluidic system could make the particles with more uniformity and stability with low cost and more convenient conditions. More research is necessary to further optimize treatment strategies for improved therapeutic outcomes with regards to *T. gondii* latent infection.

Acknowledgements

This study is a part of the MSc thesis presented by M.M. Heidari. The authors wish to thank Dr. Parvin Mohammadi and Dr. Maryam Damchi for their technical assistance.

Financial Support

This research was funded by Zanjan University of Medical Sciences with grant number A-12-245-13.

Conflict of Interest

The authors declare that there is no conflict of interests.

References

1. Dubey JP. Toxoplasmosis–a waterborne zoonosis. Vet Parasitol. 2004;126(1-2):57-72.
2. Dubey J. Advances in the life cycle of *Toxoplasma gondii*. Int J Parasitol. 1998;28(7):1019-24.
3. Dubey JP. The history and life cycle of *Toxoplasma gondii*. In: *Toxoplasma gondii*. Elsevier; 2020. p. 1-19.
4. Dickerson FB, Stallings CR, Boronow JJ, Origoni AE, Yolken RH. A double-blind trial of adjunctive azithromycin in individuals with schizophrenia who are seropositive for *Toxoplasma gondii*. Schizophr Res. 2009;112(1-3):198-9.
5. Fuglewicz AJ, Piotrowski P, Stodolak A. Relationship between toxoplasmosis and schizophrenia: a review. Adv Clin Exp Med. 2017;26(6):1031-6.
6. Hrdá Š, Votýpka J, Kodym P, Flegr J. Transient nature of *Toxoplasma gondii*-induced behavioral changes in mice. J Parasitol. 2000;86(4):657-63.
7. Firouzeh N, Ziaali N, Sheibani V, et al. Chronic *Toxoplasma gondii* infection potentiates Parkinson's disease course in mice model. Iran J Parasitol. 2021;16(4):527-537.
8. Gormley PD, Pavesio CE, Minnasian D, Lightman S. Effects of drug therapy on *Toxoplasma* cysts in an animal model of acute and chronic disease. Invest Ophthalmol Vis Sci. 1998;39(7):1171-5.
9. Walker MJ. Opportunistic infections studies update. NIAID AIDS Agenda. 1995:6-7.
10. Araujo F, Shepard R, Remington J. In vivo activity of the macrolide antibiotics azithromycin, roxithromycin and spiramycin against *Toxoplasma gondii*. Eur J Clin Microbiol Infect Dis. 1991;10:519-24.
11. Araujo FG, Guptill DR, Remington JS. Azithromycin, a macrolide antibiotic with potent activity against *Toxoplasma gondii*.

Antimicrob Agents Chemother. 1988;32(5):755-7.
12. Araujo FG, Shepard RM, Remington JS. In vivo activity of the macrolide antibiotics azithromycin, roxithromycin and spiramycin against *Toxoplasma gondii*. Eur J Clin Microbiol Infect Dis. 1991;10(6):519-24.
13. Değerli K, Kilimcioğlu AA, Kurt O, Tamay AT, Ozbilgin A. Efficacy of azithromycin in a murine toxoplasmosis model, employing a *Toxoplasma gondii* strain from Turkey. Acta Trop. 2003;88(1):45-50.
14. Chang HR. The potential role of azithromycin in the treatment or prophylaxis of toxoplasmosis. Int J STD AIDS. 1996;7 Suppl 1:18-22.
15. Caprifico AE, Foot PJ, Polycarpou E, Calabrese G. Overcoming the blood-brain barrier: Functionalised chitosan nanocarriers. Pharmaceutics. 2020; 12(11):1013.
16. Panyam J, Labhasetwar V. Biodegradable nanoparticles for drug and gene delivery to cells and tissue. Adv Drug Deliv Rev. 2003;55(3):329-47.
17. Assolini JP, Concato VM, Gonçalves MD, et al. Nanomedicine advances in toxoplasmosis: diagnostic, treatment, and vaccine applications. Parasitol Res. 2017;116:1603-15.
18. Briones E, Isabel Colino C, Lanao JM. Delivery systems to increase the selectivity of antibiotics in phagocytic cells. J Control Release. 2008;125(3):210-27.
19. Soheili S, Mandegar E, Moradikhah F, Doosti-Telgerd M, Javar HA. Experimental and numerical studies on microfluidic preparation and engineering of chitosan nanoparticles. J Drug Deliv Sci Technol. 2021;61:102268.
20. Chai Y, Wang Y, Li B, Qi W, Su R, He Z. Microfluidic synthesis of lignin/chitosan nanoparticles for the pH-responsive delivery of anticancer drugs. Langmuir. 2021;37(23):7219-26.
21. Cheraghipour K, Masoori L, Ezzatkhah F, et al. Effect of chitosan on *Toxoplasma gondii* infection: A systematic review. Parasite Epidemiol Control. 2020;11:e00189.
22. Etewa SE, El-Maaty DAA, Hamza RS, et al. Assessment of spiramycin-loaded chitosan nanoparticles treatment on acute and chronic toxoplasmosis in mice. J Parasit Dis. 2018;42:102-13.
23. El-Gendy AML, Mohammed MAA, Ghallab MMI, Aziz MOA, Ibrahim SM. Therapeutic effect of chitosan nanoparticles and metronidazole in treatment of experimentally giardiasis infected hamsters. Iran J Parasitol. 2021;16(1):32-42.
24. Hagras NA-e, Allam AF, Farag HF, et al. Successful treatment of acute experimental toxoplasmosis by spiramycin-loaded chitosan nanoparticles. Exp Parasitol. 2019;204:107717.
25. Teimouri A, Azami SJ, Keshavarz H, et al. Anti-*Toxoplasma* activity of various molecular weights and concentrations of chitosan nanoparticles on tachyzoites of RH strain. Int J Nanomedicine. 2018;13:1341-51.
26. Saraei M, Samadzadeh N, Khoeini J, et al. In vivo anti-*Toxoplasma* activity of aripiprazole. Iran J Basic Med Sci. 2015;18(9):938-41.
27. Saraei M, Ghaderi Y, Mosavi T, et al. The effect of fluphenazine and thioridazine on *Toxoplasma gondii* in vivo. Iran J Parasitol. 2016;11(2):226-231.
28. Mirhosseini M, Yazdani N, Dehghan Hamdan A. Investigation of antimicrobial properties of chitosan– ZnO nanocomposite. Razi J Med Sci. 2016;23(147):104-14.
29. Abd Elgawad H, Alhusseiny SM, Taman A, et al. Biological evaluation of newly synthesized quinoline–based compound PPQ-8 in acute and chronic toxoplasmosis: An experimental study. Exp Parasitol. 2019;206:107756.
30. Teimouri A, Motevalli Haghi A, Nateghpour M, et al. Antimalarial efficacy of low molecular weight chitosan against *Plasmodium berghei* infection in mice. J Vector Borne Dis. 2016;53(4):312-316.
31. Gaafar MR, Mady RF, . Diab RG, Shalaby ThI. Chitosan and silver nanoparticles: Promising anti-toxoplasma agents. Exp Parasitol. 2014; 143:30-38.
32. Rahimi Esboei B, Keighobadi M, Ziaei Hezarjaribi H, et al. Promising *in vitro* anti-*Toxoplasma gondii* effects of commercial

chitosan. Infect Disord Drug Targets. 2021; 21(1):151-155.
33. Raouf M, Essa S, El Achy S, et al. Evaluation of Combined Ciprofloxacin and azithromycin free and nano formulations to control biofilm producing *Pseudomonas aeruginosa* isolated from burn wounds. Indian J Med Microbiol. 2021;39(1):81-7.
34. Jonassen H, Kjøniksen A-L, Hiorth M. Stability of chitosan nanoparticles cross-linked with tripolyphosphate. Biomacromolecules. 2012;13(11):3747-56.
35. Habibizadeh M, Nadri S, Fattahi A, et al. Surface modification of neurotrophin-3 loaded PCL/chitosan nanofiber/net by alginate hydrogel microlayer for enhanced biocompatibility in neural tissue engineering. J Biomed Mater Res A. 2021;109(11):2237-54.
36. Dumas JL, Chang R, Mermillod B, et al. Evaluation of the efficacy of prolonged administration of azithromycin in a murine model of chronic toxoplasmosis. J Antimicrob Chemother. 1994;34(1):111-8.
37. Asgari Q, Keshavarz H, Shojaee S, et al. In vitro and in vivo potential of RH strain of *Toxoplasma gondii* (Type I) in tissue cyst forming. Iran J Parasitol. 2013;8(3):367-75.
38. Salimi M, Shojaee S, Keshavarz H, Mohebali M. Cyst formation from virulent RH strain of *Toxoplasma gondii* tachyzoite: in vitro cultivation. Iran J Parasitol. 2016;11(1):81-5.
39. Djurković-Djaković O, Milenković V, Nikolić A, et al. Efficacy of atovaquone combined with clindamycin against murine infection with a cystogenic (Me49) strain of *Toxoplasma gondii*. J Antimicrob Chemother. 2002;50(6):981-7.
40. Ferreira RA, Oliveira AB, Ribeiro MF, et al. *Toxoplasma gondii*: in vitro and in vivo activities of the hydroxynaphthoquinone 2-hydroxy-3-(1'-propen-3-phenyl)-1, 4-naphthoquinone alone or combined with sulfadiazine. Exp Parasitol. 2006; 113(2):125-9.
41. Shu H, Jiang L. Effect of garlicin and minocycline on the cyst formation of *Toxoplasma gondii* in mice. Chinese J Zoonoses. 2002;18(1):100-1.
42. Ferguson D, Huskinson-Mark J, Araujo F, Remington J. An ultrastructural study of the effect of treatment with atovaquone in brains of mice chronically infected with the ME49 strain of *Toxoplasma gondii*. Int J Exp Pathol. 1994;75(2):111-6.
43. Rutaganira FU, Barks J, Dhason MS, et al. Inhibition of calcium dependent protein kinase 1 (CDPK1) by pyrazolopyrimidine analogs decreases establishment and reoccurrence of central nervous system disease by *Toxoplasma gondii*. J Med Chem. 2017;60(24):9976-89.
44. Mahmoud DM, Mahmoud MS, Ezz-El-Din HM, et al. Artesunate effect on RH virulent and ME49 non-virulent strains of *Toxoplasma gondii*: in vitro and in vivo experimental studies. Sci Parasitol. 2016;17:83-92.
45. Chew WK, Segarra I, Ambu S, Mak JW. Significant reduction of brain cysts caused by *Toxoplasma gondii* after treatment with spiramycin coadministered with metronidazole in a mouse model of chronic toxoplasmosis. Antimicrob Agents Chemother. 2012;56(4):1762-8.
46. Ghaffarifar F, Pour MA, Sharifi Z, Asl AD, Al-Kawaz E. The effect of vitamin D3 alone and mixed with IFN-γ on tachyzoites of *Toxoplasma gondii* (RH strain) proliferation and nitric oxide (NO) production in infected macrophages of BALB/C mice. Iran J Parasitol. 2010;5(3):48-56.